# Compact Methodology for Computing Limit-Cycle Oscillations in Aeroelasticity

Bogdan I. Epureanu*
*University of Michigan, Ann Arbor, Michigan 48109*
and
Earl H. Dowell[†]
*Duke University, Durham, North Carolina 27708*

A technique for computing limit-cycle oscillations of aeroelastic systems is presented. This technique can be used also for constructing and identifying reduced-order models that characterize accurately limit-cycle oscillations. The models presented use a spatial model reduction combined with a nonlinear identification technique. The finite difference in time method, a methodology similar to a finite element in time, is discussed. The specific novel aspects of the proposed method are noted. Numerical examples analyzing the dynamics of a panel forced by a buffeting aerodynamic load demonstrate the performance of the proposed methods.

## Nomenclature

| | | |
|---|---|---|
| $A$ | = | coefficient of mass distribution for the panel, considered constant |
| $B$ | = | coefficient of fluid-induced damping, $B = \rho U/\text{Mach}$ |
| $b_i(\tau)$ | = | basis functions for the finite difference in time method |
| $C$ | = | two-point correlation matrix |
| $C_i$ | = | zeroth-order system parameters |
| $c_k$ | = | Fourier coefficients |
| $F(Q)$ | = | nonlinear vector function of dimension $m$ |
| $f$ | = | nonlinear function of dimension $n$ |
| $G$ | = | coefficient of tension induced by bending |
| $H$ | = | coefficient of aerodynamic convection, $H = \rho U^2/M$ |
| $H_{i,j,k}$ | = | second-order system parameters |
| $J_{i,j}$ | = | first-order system parameters |
| $L$ | = | size of the state-space vector |
| $M$ | = | number of snapshots |
| $m$ | = | dimension of the reduced-order model |
| $N$ | = | number of modes/frequencies/sample points |
| $n$ | = | number of time instants during a period |
| $P$ | = | in-plane load on the panel |
| $Q$ | = | coordinates of the reduced-order model |
| $q$ | = | external forcing distributed along the panel |
| $T$ | = | period of a periodic solution |
| $T_{i,j,k,p}$ | = | third-order system parameters |
| $t, \tau$ | = | time |
| $U$ | = | flow velocity |
| $v_i$ | = | eigenvectors of the correlation matrix $C$ |
| $w$ | = | bending deformation |
| $X$ | = | state-space vector |
| $x$ | = | coordinate along the panel |
| $x$ | = | vector of unknowns |
| $x_p(t)$ | = | periodic solution |
| $\Delta$ | = | inverse of the period $T$ |
| $\lambda_i$ | = | eigenvalues of the correlation matrix $C$ |
| $\xi$ | = | nondimensional time fraction |
| $\rho$ | = | flow density |

## Introduction

THIS research is concerned with the modeling of typically high-dimensional aeroelastic systems. Many design and control applications in aeroelasticity require relatively simple models to predict the dynamics of aeroelastic systems with as little computational and experimental effort as possible. Reducing the complexity of these models is critical in many applications and has not been widely investigated for the case of strongly nonlinear and/or chaotic systems. In such cases an important aspect of the nonlinear dynamics is the presence of limit-cycle oscillations. In this paper we present a technique for constructing and identifying reduced-order models, which accurately characterize limit-cycle oscillations of aeroelastic systems. The models presented use a spatial model reduction based upon proper orthogonal decomposition (POD)[1,2] combined with a nonlinear identification technique. The nonlinear identification methodology employs a least-squares method in the proper orthogonal vector space, that is, a reduced space. The calculation of the limit-cycle oscillations is done by means of a finite difference in time approach (FDTA), similar to the finite element in time approach.[3−10]

Most recent research on reduced-order modeling has been focused on linearized systems. However, time-linearized techniques have been used by Noor[11] and Stone and cutler[12] to model both linear and nonlinear phenomena. The linearized reduced-order modeling technique has been applied to a wide variety of systems, such as Burger's model of turbulence,[13−15] Euler equations, Navier–Stokes equations, Raleigh–Bénard convection,[16] turbulence, and boundary-layer models.[17] Fully nonlinear normal modes and reduced-order models have been investigated also for low-dimensional systems by Shaw and Pierre.[18] The nonlinear normal modes have been shown also to be difficult to compute and interpret for high-dimensional systems. Recently, Dowell and Hall[1] have prepared a review of eigenmode and POD-based reduced-order models for linear and nonlinear aerodynamics of high-dimensional systems, which summarizes and discusses much of the relevant literature and recent research advances. The techniques presented in this paper are distinct from previous research in that they focus on a combination of a simultaneous model reduction and system identification especially designed for limit-cycle calculation using a FDTA computational method.

There are several techniques for computing limit-cycle oscillations of nonlinear systems. These techniques are based on time integration or harmonic balance in the frequency domain. Several variations of the harmonic balance method (HBM) have been presented

in the literature. Methods such as the classical and the incremental HBM[19] use the direct Fourier transform, thus requiring extensive analytical work prior to implementation. Other methods such as the fast Galerkin[20] and the alternating frequency-time domain technique use the fast Fourier transform instead of the direct Fourier transform, and they have been shown to be more efficient computationally, more general, and easier to implement. Common to all of these methods is that the original, time domain equations describing the dynamics are transformed to an alternate vector space, that is, the Fourier space. The transformed set of equations is then truncated, and a finite set of nonlinear algebraic equations is obtained. The unknowns in these equations are typically Fourier coefficients, and they are solved by an iterative method such as Newton–Raphson, Broyden, etc. In this paper we present an alternate approach to the Fourier transform. The fundamental idea of transforming the initial set of differential equations to a set of discrete algebraic equations is maintained. However, the set of basis functions used for the transformation are not sinusoidal in time but different, more general functions. Also, the algebraic equations obtained after the transformation of the differential equations of the dynamics are solved in the time domain rather than the frequency domain.

The HBM has been applied to a wide variety of problems and is one of the most frequently used techniques to study periodic solutions of nonlinear dynamical systems, that is, limit-cycle oscillations or forced responses. Computing the periodic solutions of nonlinear dynamical systems[21−25] is critical for analysis, design, and control applications.[26−28] Thus, the HBM has been studied by researchers analyzing a broad range of fundamental problems such as predicting chaos,[29] limit-cycle oscillations,[30−34] and many other applications.[35−39] Hall et al.[40] have developed a novel approach for the nonlinear dynamics of high-dimensional aerodynamic models that is broadly similar to the HBM; a more detailed discussion has been presented by Dowell and Hall.[1]

The first step to be performed when using the HBM to determine a periodic solution of a system of nonlinear differential equations is to construct the harmonically balanced equations. The second step is to solve the resulting nonlinear equations. These equations have been solved in the literature using a wide variety of numerical techniques. The most frequently used techniques are the incremental HBM,[41−43] the Newton–Raphson, and the Broyden methods. In some cases these methods are used in conjunction with a continuation method,[44,45] because they are often highly nonlinear and have multiple solutions.

Since the early successful attempts to apply the HBM, most researchers have formulated the harmonic balance equations analytically, as part of their model.[46,47] This approach has the drawback of being rather difficult to apply to high-dimensional systems because of the extensive algebra involved, especially when a multifrequency HBM is employed. To automate the calculation of the frequency domain equations, some researchers have used symbolic computation techniques,[48] whereas others have developed numerical algorithms that can be applied to a certain category of problems.[49,50]

To alleviate this difficulty, alternate implementations of the HBM based on the fast Fourier transform of the nonlinear system of equations have been proposed. These approaches are more easily extended to a wider variety of systems and, in some cases, do not require an analytic generation of the harmonic balance equations. Choi and Noah[51] have used the fast Fourier transform and the alternating frequency-time domain technique applied to piece-wise linear systems. However, their implementation requires extensive analytical calculations when the nonlinearities present in the system are more complex. Cameron and Griffin[52] have investigated an iterative method used in conjunction with the HBM and have presented a comparison between the Broyden method and the Newton–Raphson method. The HBM has been used also with an alternating frequency-time domain method, an extension of the fast Galerkin technique presented by Ling and Wu.[20] Aprile et al.[53] have presented a generalized alternating frequency-time domain method. Also, the nonlinear frequency domain Broyden and Newton–Raphson iterations have been compared to time domain methods such as the Newmark integration.

In this paper the standard multifrequency HBM is discussed, and an alternate approach (i.e., the FDTA) is proposed. The specific novel aspects of the proposed method are presented. An aeroelastic example analyzing the dynamics of a panel forced by a buffeting aerodynamic load is presented to demonstrate the performance of the proposed method.

## Model Reduction Methodology

Herein, the approach used to address the complexity caused by the spatial distribution of the aeroelastic system is based upon POD.[1,54,55] This approach requires the simulation or the measurement of the dynamics of the system of interest over a time interval. A model for the spatial coherence of the dynamics is then constructed based on this observation. For linear systems the models obtained using POD are similar to models based on modal analyses. The performance of the POD is nevertheless influenced by the level of modal coupling caused by nonlinear phenomena. And, of course, one can use linear modes as basis functions to represent nonlinear phenomena; however, the nonlinear effects will lead to coupling of these modes even though they are eigenmodes.

In the POD method[1,54,55] the response of the system of interest is obtained by time marching and stored in a state-space vector solution $X_i$ for a set of $M$ time instants, that is, $i = 1, \ldots, M$. Each solution vector $X_i$ has $L$ entries, where $L$ represents the size of the state space of the system. A matrix $R$ of size $L \times M$ is formed such that its $i$th column is the solution vector $X_i$ for each $i = 1, \ldots, M$. A correlation matrix is then assembled of the form

$$C = R^T R \tag{1}$$

where the superscript $T$ indicates the transpose. The eigenvalues of the correlation matrix are then obtained by solving an eigenvalue problem of dimension $M \times M$, that is,

$$Cv_i = \lambda_i v_i \tag{2}$$

Among the eigenvalues obtained, the largest eigenmodes contain most of the energy of the aeroelastic system. The reduced-order modes $v_i$ and eigenvalues are, therefore, organized in descending order, that is, from the most important to the least important. The most significant $m$ modes are then grouped in a matrix $V$ of size $M \times L$ such that the $i$th column of $V$ is the vector $v_i$, with $i = 1, \ldots, m$. The equations of motion and the state-space vector $X$ are then projected onto the space spanned by the vectors $v_i$ (with $i = 1, \ldots, m$), and a reduced-order model is obtained. The state-space vector of the reduced-order model is a vector $\tilde{X}$ of (small) size $m$. The state-space vector $X$ is approximated by $X = P\tilde{X}$, where the matrix $P$ is given by $P = RV$.

The approach used for addressing the temporal complexity of the dynamics is based upon a local system identification of limit-cycle oscillations.[26] The local system identification method is an identification technique designed for determining the dynamical models of systems undergoing limit-cycle oscillations. The local identification method has been tested for low-dimensional systems and has been shown to be a versatile and accurate method.[26] The tests that have been done for low-dimensional systems have indicated that the method can be attractive for the identification of larger dimensional systems, and its performance in the latter case is discussed herein. The example used for testing the identified reduced-order models is a numerical simulation of an aeroelastic system composed of a panel forced by a buffeting aerodynamic load.

The end results are low-dimensional models capable of predicting accurately the dynamics of large, spatially distributed nonlinear systems in the neighborhood of a limit-cycle oscillation in phase space. The entire identification and model reduction procedure can be summarized in four steps. First, time series of measurable dynamic variables are obtained from numerical computations or experiments. Second, POD is used to identify coherent structures embedded in the time series. Third, the dominant coherent structures are used to construct a reduced-order model that is dependent on unknown parameters. Fourth, the dynamics of the coherent structures is extracted from the time series and used for identifying the

reduced-order model (i.e., the unknown parameters of the reduced-order model are identified).

POD provides a set of basis vectors that characterize the coherent structures. However, POD does not provide a model per se unless we reconstruct the original mathematical model in terms of POD basis functions,[1,54,55] or, as shown in the present paper, use system identification techniques to identify the parameters of the reduced-order model from numerical or experimental data. Using the latter approach, a reduced-order model can be obtained by considering a general functional form of the model that depends on several parameters, and then identifying these parameters, as shown in the following sections.

## Standard Harmonic Balance Method

The standard HBM is designed to determine approximately the periodic solutions of a system of nonlinear ordinary differential equations describing the dynamics of a system

$$f(x, \dot{x}, \ddot{x}, \ldots, t) = 0 \qquad (3)$$

where $f$ is a $n$-dimensional nonlinear function dependent on the vector of unknowns $x$, its time derivatives $\dot{x}$, $\ddot{x}$, etc., and the time $t$. The period $T$ of a periodic solution $x_p$ is most often assumed known, and the solution is written as a Fourier series

$$x_p(t) = \sum_{k=-\infty}^{\infty} c_k e^{k\omega t j} \qquad (4)$$

where $\omega = 2\pi/T$ is the fundamental frequency and $j = \sqrt{(-1)}$. The Fourier coefficients have complex conjugate values $c_k = c_{-k}^*$ when the state vector $x$ is real.

The essence of the HBM is to truncate the series in Eq. (4) to a finite number of modes $N$ and then substitute it into Eq. (3). Then, one extracts analytically or numerically (by means of a Fourier transform) the coefficients multiplying the terms $e^{i\omega t j}$ for all $i = 0 \ldots N$ from the newly obtained expression and sets them to zero, obtaining

$$g_i(T, c_0, \ldots, c_N) = 0 \qquad (5)$$

with the coefficients $c_{-k}$ appropriately substituted for $c_k^*$ for all $k = 1 \ldots N$. One therefore determines a set of $N + 1$ nonlinear vector equations in the frequency domain that must be solved for the unknown coefficients $c_k$, $k = 0 \ldots N$. The Newton–Raphson technique and the incremental HBM are the methods most often applied to determine the Fourier coefficients from Eq. (5) of the truncated series that approximates $x_p$. When the period $T$ of the limit cycle is unknown, one can use the same equations by fixing the value of one of the coefficients $c_k$ and solving for the period $T$ along with the remaining $N$ coefficients.[20] Some researchers derive analytical expressions for Eq. (5) for simple systems.[46,47] However, Eq. (5) is obtained most often numerically rather than analytically because of the complexity of the Fourier transform of the nonlinearities.

Obtaining Eq. (5) for given values of the Fourier coefficients $c_k$ is a difficult and computationally expensive step in the implementation of the HBM. One approach to reduce the computational time is to compute a time series of $f$, perform a fast Fourier transform of this series, and extract a number of $N + 1$ Fourier coefficients of $f$. Then, these $N + 1$ Fourier coefficients are used to complete the HBM. When the solution of Eq. (5) is obtained, the $N + 1$ values of $g_i$ are approximately zero. They are considered the residual in the iterative nonlinear solver used. Additionally, to implement several nonlinear solvers such as a standard Newton–Raphson technique one must compute the Jacobian matrix, which contains the derivatives of $g_i$ with respect to $c_k$.[56] For complex functions $f$ such as numerically known functions, the transformation of Eq. (5) to the time domain can be simplified by using fast Fourier transforms, for example. Nevertheless, such transformations are computationally intensive, and their frequent evaluation leads to significantly longer computation time when compared to the finite element in time method discussed by Warner and Hodges[9,10] or the FDTA presented in the next section.

The nonlinear equations obtained in the frequency domain are complex and frequently do not have a simple analytical expression. Thus, most often general purpose nonlinear solvers are used to determine the solution of these equations. Several researchers[20,52] have investigated the Newton–Raphson approach and the Broyden method[52] for the alternating frequency-time domain method. They suggest that these methods fail under certain circumstances and that more robust algorithms should be used. However, the problem caused by the nonlinearities is still not solved completely. Indeed, even the most robust techniques available might fail to converge if the initial guess for a solution is not close enough to the exact solution.[57] In this paper we focus on the fundamental aspect of the method employed rather than on the specific nonlinear solver used. The FDTA is presented in the following section as an alternative approach to the frequency domain method or classical time integration.

## Finite Difference in Time Approach

One of the basic steps performed in the HBM is to approximate the solution of the differential equation of the dynamics [Eq. (3)] by a linear combination of complex exponential or sinusoidal functions. We propose an alternate method. Instead of using complex exponentials, we propose a different set of linearly independent basis functions. These basis functions are denoted by $b_k(\tau)$ and are functions of the nondimensional time $\tau$, where $\tau = t/T$, with $T$ being the period of the limit cycle to be computed. For the present discussion the exact shape of the basis functions is considered fixed. The rationale for calling the proposed technique a FDTA is discussed in the next section.

Similar to the standard HBM, the solution of Eq. (3) can be approximated by

$$x_p(t) = \sum_{k=-\infty}^{\infty} c_k b_k\left(\frac{t}{T}\right) \qquad (6)$$

where $c_k$ are unknown vector coefficients. When the period of the limit cycle to be computed is not known, the variable $T$ is also unknown. The series on the right-hand side of Eq. (6) is then truncated to a finite number of modes $N$ and substituted into Eq. (3). The time derivatives of the unknown vector $x_p$ are computed based on the truncated series. For example, the first-order derivative of $x_p$ can be expressed as

$$\dot{x}_p(t) = \frac{1}{T} \sum_{k=0}^{N} c_k \dot{b}_k\left(\frac{t}{T}\right) \qquad (7)$$

Substituting Eq. (7) in Eq. (3), one obtains a set of $N$ equations for the unknown coefficients $c_i$ multiplying each basis function $b_i$ for all $i = 0 \ldots N$. Similar to Eq. (5), one obtains

$$h_i(T, c_0, \ldots, c_N) = 0 \qquad (8)$$

Distinct from the HBM-type approaches, in the FDTA the basis functions are not necessarily orthogonal although they are linearly independent. Thus, Eq. (8) is not obtained by collecting the coefficients multiplying the basis functions and setting these coefficients to zero (to be explained in the next section). But indeed Eq. (8) is an equation for the coefficients $c_i$ and the period $T$, that is, coordinates of $x_p$ in the transformed space. However, Eq. (8) is expressed in the time domain and not in the transformed domain. The HBM is based on Eq. (5) where all terms are expressed in the transformed space, that is, the frequency domain. The difference between Eqs. (8) and (5) is one of the fundamental differences between the FDTA and the HBM.

Another substantial difference between the FDTA and the HBM is that, by operating in the time domain instead of the transformed space, the nonlinearities, the forcing terms and other aspects of the model formally expressed by Eq. (3) are much easier to handle computationally. Additionally, the transformations between the time domain and the transformed space are not required. Specifically, in the standard HBM one direct Fourier transform (or FFT) is needed to determine the residual vector in the frequency domain [Eq. (5)] starting from the current limit-cycle approximation $x$ in the time domain. Also, an inverse Fourier transform (or FFT) is

needed at each iteration to update the limit-cycle approximation $x$ in the time domain based on the iteration step obtained from Eq. (5) in the frequency domain. Neither the direct nor the inverse Fourier transforms (or FFTs) are required in the FDTA.

Equation (6) does not depend explicitly on $T$ because each basis function $b_k(\tau)$ does not depend explicitly on $T$. Each basis function is specified for $\tau$ between zero and one, wherein $t/T$ lies. This implies that the shape of the basis function is independent of the period $T$, that is, the basis functions are independent of the timescale used. In the next section we propose a set of basis functions and describe in more detail how these basis functions provide a more efficient path to the expression for Eq. (8).

## Basis Functions

Distinct from the HBM, we consider as unknowns the values of $x$ at specific time instants. This is equivalent to considering as basis functions a set of interpolation functions. For simplicity and without any loss of generality, the interpolation functions are chosen to be second order. Of course, the decision as to whether a first-, second-, or a higher-order interpolation should be used is dependent upon the particular application and the order of the differential equation of the dynamics, Eq. (3).

The time values that define the unknowns are denoted by $t_i$. Also, each basis function $b_i$ is defined as a second-order interpolation function for the time interval $[t_{i-1}; t_{i+1}]$, that is,

$$b_i(\tau) = \begin{cases} 0, & \tau \leq t_{i-1}/T \\ q_i(\xi), & t_{i-1}/T \leq \tau \leq t_{i+1}/T \\ 0, & \tau \geq t_{i+1}/T \end{cases} \quad (9)$$

where the time fraction $\xi$ is given by $(\tau T - t_{i-1})/(t_{i+1} - t_{i-1})$. The functions $q_i(\xi)$ can be considered quadratic interpolation functions of the nondimensional fraction of time $\xi$. For simplicity, we consider that the time values $t_i$ are uniformly distributed between zero and $T$, that is, $t_i = [(i-1)/(N-1)]T$, so that the nondimensional time values $\tau_i$ are 0, $1/(N-1)$, $2/(N-1)$, ..., $(N-2)/(N-1)$, 1. The quadratic interpolation functions are considered to satisfy $c_i q_i(0) = x_p(t_{i-1})$, $c_i q_i(\frac{1}{2}) = x_p(t_i)$, and $c_i q_i(1) = x_p(t_{i+1})$. Thus, the first- and second-order derivatives of $x_p$ are evaluated using a centered finite difference. For a uniformly distributed set of values $\tau_i$, Eq. (7) can be expressed as

$$\dot{x}_p(t_i) = [(N-1)/T]\{[x_p(t_{i+1}) - x_p(t_{i-1})]/2\} \quad (10)$$

In a state-space formulation it is not necessary to approximate the second- and higher-order derivatives using finite differences. Nevertheless, a state-space formulation leads to a larger number of unknowns (as velocities are unknown). An alternate method, which does not increase the number of unknowns, is to approximate the second- and higher-order derivatives in time using a standard finite difference approach. Thus, the second-order derivative of $x_p$ can be expressed as

$$\ddot{x}_p(t_i) = [(N-1)/T]\{[\dot{x}_p(t_{i+1}) - \dot{x}_p(t_{i-1})]/2\}$$

$$= [(N-1)/T]^2\{[x_p(t_{i+1}) - 2x_p(t_i) + x_p(t_{i-1})]/4\} \quad (11)$$

where $\dot{x}_p(t_i)$ are given by Eq (10). The specific choice of interpolation functions determines the highest level of nonzero derivative, which is possible to model. For example, the second-order interpolation with uniform distribution of $\tau_i$ models nonzero derivatives up to second order. Moreover, the time intervals used for discretization do not have to be of equal length, although in the examples provided we considered equal length time intervals for simplicity.

Substituting Eqs. (10) and (11) into the differential equation of the dynamics [Eq. (3)], one obtains a set of $N$ vector equations for the $N$ values of $\tau_i$, that is,

where $\Delta$ is the inverse of the period $\Delta = 1/T$. For each value of $\tau_i$, one obtains $n$ equations from Eq. (12), which amount to a total of $n \times N$ equations. The unknowns are the $N$ values of the vector $x_p(t_i)$ of size $n$, that is, a total of $n \times N$ unknowns. When the value of the period $T$ is known, the coefficient $\Delta$ is known, and the $n \times N$ can be solved for the $n \times N$ unknowns. Additionally, the values $x_p(t_0)$ and $x_p(t_{N+1})$ required when the index $i$ is 1 or $N$ are easily expressed based on the periodicity of the limit cycle, that is, $x_p(t_0) = x_p(t_{N-1})$ and $x_p(t_{N+1}) = x_p(t_2)$. These equalities are used in Eq. (12) to express $x_p(t_0)$ and $x_p(t_{N+1})$ in function of the unknowns $x_p(t_i)$, where $i$ varies from 1 to $N$. When the period $T$ of the limit cycle is unknown, there are $n \times N + 1$ unknowns to be solved for. The equations used are the same $n \times N$ equations obtained using Eq. (12) for $i$ from 1 to $N$. In addition, the $(n \times N + 1)$th necessary equation is obtained by imposing a given value to one of the variables $x_{p_i}(t_j)$ or its time derivative $\dot{x}_{p_i}(t_j)$, which requires a priori knowledge of the system properties. However, this knowledge is commonly available. For example, one usually knows that a variable (such as a position coordinate at location $i$) is zero at some unknown instant during the motion. In such a case one sets $x_{p_i}(t_j)$ to zero for $j = 1$. The index $j$ can be chosen 1 or any arbitrary value $(j \leq N)$ because its role is simply to set the phase of the limit cycle computed. The same limit cycle is obtained for distinct values of $j$, although the phase of the limit cycle varies with $j$.

When a nonuniform distribution of the time values $t_i$ is used, then Eq. (12) has a different form because the finite differences in Eq. (10) are not centered finite differences, and the derivatives at time $t_i$ depend not only on the values of the unknowns $x_p(t_{i+1})$ and $x_p(t_{i-1})$, but also on $x_p(t_i)$. However, these features do not affect the general approach or the simplicity of the method.

An important advantage of the FDTA over the HBM is the fact that the Jacobian $\partial f/\partial x_p(t_i)$ necessary to solve Eq. (12) is highly structured and sparse. The Jacobian is a block $s$ diagonal, where $s$ is the size of the highest order finite difference stencil used to approximate time derivatives. For the example problem discussed in the following, the Jacobian is block tridiagonal. The size of each block is equal to the size of the vector $x_p$, that is, the number of coordinates. The favorable structure of the Jacobian overcomes the problem commonly encountered in the standard HBM where the Jacobian is full (not sparse) and increases in size as the square of the number of coordinates and frequencies used. Thus, the advantage of the proposed method over the standard HBM is two-fold. First, the Jacobian is easy to compute as it is sparse, requires few computations, and can be implemented in a simple numerical or analytical routine. Second, the solution of the linear set of equations necessary for a Newton–Raphson (or other) iterative solver can easily be computed because fast and simple routines for solving linear systems with block banded matrices are widely available. When the period $T$ of the limit cycle is unknown, the structure of the Jacobian is modified slightly. One additional full column and one additional (simple and sparse) row are added. Nevertheless, simple methods from linear algebra are available for dealing with this issue.[58]

The FDTA is a time-based method, and the final results bear a strong similarity to the finite element in time approach.[9,10] However, distinct from the finite element in time approach, the present method uses finite differences rather than finite elements. Thus, in the FDTA there is no appeal to a variational principle per se,[59] although the limit-cycle oscillations are computed using the original differential equations in time directly.

## Panel Forced by Buffeting Aerodynamic Loads

The nonlinear aeroelastic system used for testing the methodology presented in the preceding section is a panel responding to a buffeting aerodynamic flow.[60] The differential equation governing the dynamics of the panel can be obtained using piston theory for modeling the aerodynamic loads caused by panel motion and

$$f\left[x_p(t_i), \frac{x_p(t_{i+1}) - x_p(t_{i-1})}{2}\Delta, \frac{x_p(t_{i+1}) - 2x_p(t_i) + x_p(t_{i-1})}{4}\Delta^2, \dots, \frac{\tau_i}{\Delta}\right] = 0 \quad (12)$$

classical plate theory for modeling the panel. The partial differential equations governing the dynamics of aeroelastic system can be expressed as

$$w''''(x, t) - Pw''(x, t) - G\left[\int_0^1 w'^2(\xi, t)\, d\xi\right] w''(x, t)$$

$$+ Hw'(x, t) + A\ddot{w}(x, t) + B\dot{w}(x, t) = q(x, t) \equiv q^+ - q^-$$

(13)

where $x$ varies from 0 to 1 and $q$ is an external forcing caused by a buffeting pressure fluctuation across the panel caused by an additional external aerodynamic forcing (i. e., $q$ is proportional to the local pressure difference across the panel). The superscripts $+$ and $-$ indicate the lower and upper sides of the panel. The prime indicates spatial derivatives, and the dot indicates time derivatives. A sketch of the panel is shown in Fig. 1.

The coefficient $G$ in Eq. (13) characterizes the nonlinear tension stiffness of the panel induced by bending deformation $w$ and is a function of the modulus of elasticity of the material and the thickness of the panel. The numerical values used for the coefficients in Eq. (13) are $A = 1$, $B = 3.87$, $G = 5.62$, $H = 150$, and $T = 0.25$. These values are chosen based on previous numerical results presented in the literature,[60] such that they characterize a plate that might undergo limit-cycle oscillations, chaotic dynamics, and stable buckling. Each of these types of dynamics is obtained for distinct values of the parameter $P$, which characterizes the in-plane load applied externally to the panel in the $x$ direction. Specifically, this parameter is set to 49.35 when investigating the case of forced or free limit-cycle oscillations, to 20 when studying stable oscillations, and to 100 when discussing chaotic dynamics. Also, the forcing magnitude $q_0$ is set to 350 when investigating forced oscillations.

Equation (13) is discretized in space using a second-order finite difference scheme. Steady-state or static solutions are computed first. The importance of the nonlinear terms in Eq. (13) is shown by the significant difference between the steady-state linear and nonlinear solutions. Shown in Fig. 2 are the steady-state panel shapes for the nonlinear model and also for the linearized model where $G$ is zero. The unsteady discretized equations are then integrated in time starting at rest from the steady state, that is, $w(x, t = 0) = w(x)_{\text{steady}}$ and $\dot{w}(x, t = 0) = 0$. An unsteady pressure difference across the
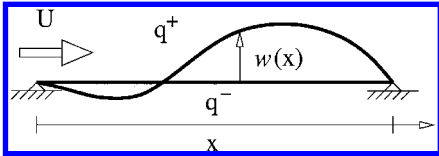


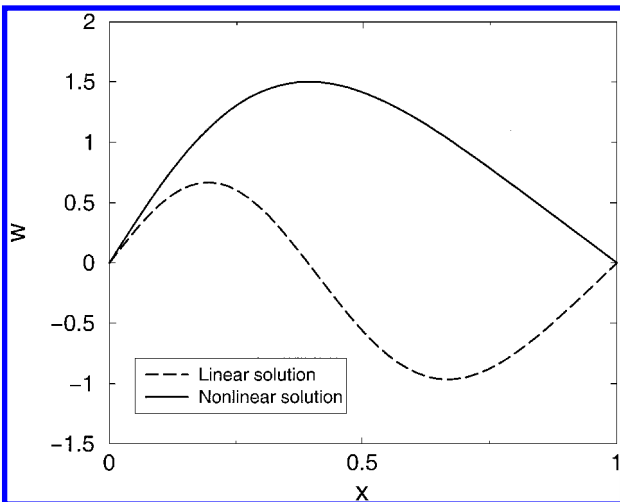Fig. 1  Panel forced by a buffeting aerodynamic load.



Fig. 2  Steady solution for the linear and nonlinear models for an in-plane load characterized by a coefficient $P$ of 49.35.
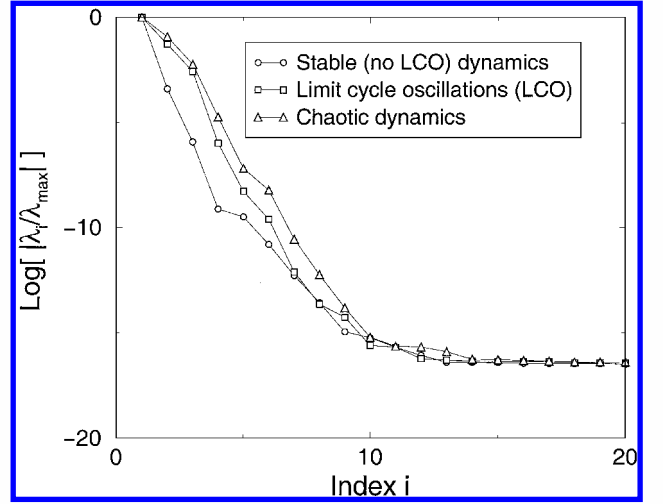


Fig. 3  Eigenvalues of the correlation matrix computed for a case of a stable panel, a limit-cycle oscillation, and a chaotic panel dynamics.
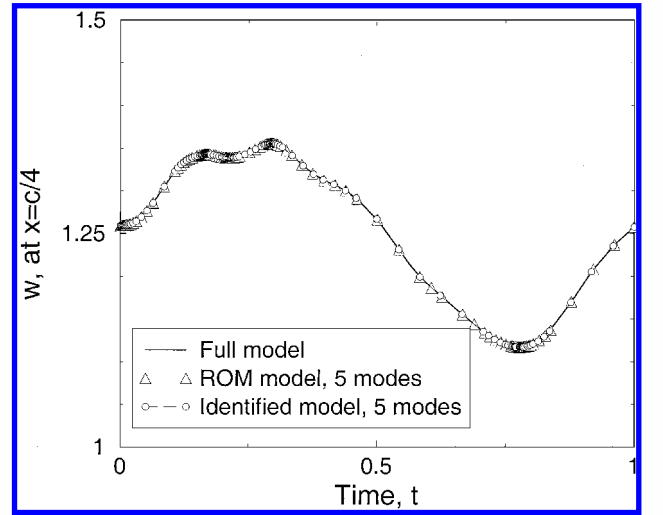


Fig. 4  Time-marching solution for a panel forced with unsteady loads using the full model, the reduced-order model, and the identified reduced-order model with five modes.

panel is applied when forced oscillations are investigated, that is, $q(x, t) = q_0[1 + 0.5 \sin(2\pi t / T)] = q^+ - q^- \neq 0$.

The deformation of the panel can be modeled in various ways. For example, finite elements (in space) or finite differences can be used to discretize Eq. (13) in space. Nevertheless, these approaches lead to very large discrete models, which include values of $w$ at many $x$ locations along the panel. However, the shapes of the panel are few and coherent. Herein, POD is used and confirms the existence of these coherent structures. Snapshots of a position along the panel at $M = 100$ time instants from time 0 to 1 are collected. The existence of spatial coherence and dominant modes, a fundamental requirement for the applicability of model reduction, is confirmed by computing the eigenvalues of the two-point correlation matrix $C$ obtained using the 100 snapshots. Figure 3 shows that only a few of these eigenvalues are large, indicating the existence of a few dominant coherent structures. The existence of these dominant structures is confirmed also by constructing several reduced-order models with 3, 5, and 15 deg of freedom. The reduced-order models are integrated in time, and the results obtained agree very well with those using the full model, as shown in Fig. 4, where $P$ is 49.35 and $q_0$ is 350, and Fig. 5, where $P$ is 20 and $q_0$ is zero. For clarity, the numerical results present the displacement at the quarter-length point of the panel only, that is, $w(x = 0.25, t)$. Nevertheless, similar results are obtained at all other locations along the panel.

A local system identification can be used to identify the reduced-order models just discussed when experimental data are available.
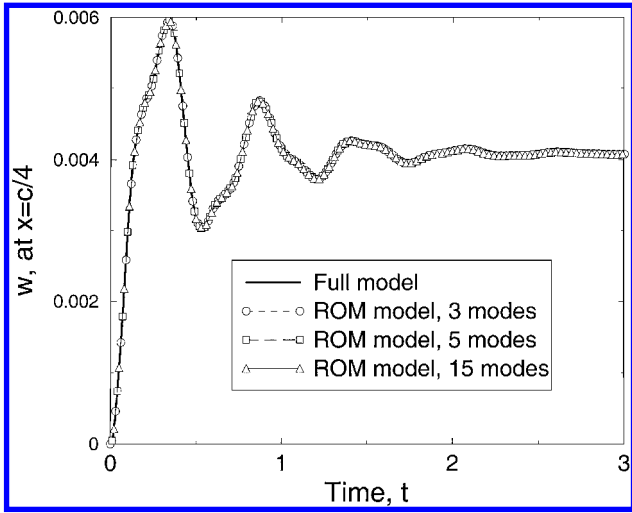
**Fig. 5 Time-marching solution for a panel using the full model and three distinct reduced-order models for a case of a stable (no limit-cycle oscillations) panel dynamics.**

To simulate this approach, one first chooses a functional form for the model of the time evolution of the system. This form is based upon the known form of the governing structural and fluid theoretical models, that is, Eq. (13) The form chosen herein is a vector polynomial of degree three, which models the nonlinear state equation and forcing as

$$F_i(Q) = C_i + J_{i,j}Q_j + H_{i,j,k}Q_jQ_k + T_{i,j,k,p}Q_jQ_kQ_p \quad (14)$$

where $F(Q)$ is a nonlinear vector function of dimension $m$ containing all spatial derivative terms in Eq. (13), and $Q$ is a vector of dimension $m$ representing the $m$ coordinates of the reduced-order model, that is, modal coordinates, also referred to as POD coordinates. All indexes $i$, $j$, $k$, $p$ vary from one to $m$, and all double indexes indicate summation. All of the coefficients $C_i$, $J_{i,j}$, $H_{i,j,k}$, and $T_{i,j,k,p}$ are constant in time, and they are obtained by means of a system identification, as follows.

Next, the parameters of the model shown in Eq. (14) can be identified based on experimental data. To simulate these data, one can collect time series for $w$ at a number of 50 locations along the panel in the $x$ direction. These locations are uniformly distributed from $x = 0$ to 1. In addition, the time series contains information only for the deflection of the panel $w$, but not its velocity. The velocity is determined by using finite differences. A local identification of the dynamics is used. Moreover, to simulate noise in the data a random perturbation of 1% is introduced. For each location along the panel, 1000 values are collected at time instants distributed uniformly from time 0 to 1. These values are used to form an overdetermined set of linear equations for the coefficients to be identified. This system of equations is solved for the unknown system coefficients, $C_i$, $J_{i,j}$, $H_{i,j,k}$, and $T_{i,j,k,p}$. For each of the 1000 sets of measured coordinates, $m$ equations are constructed. For the calculation presented in Fig. 4, a set of $1000 \times m = 5000$ linear equations are formed and solved using the least-squares method for the total number of unknowns $m^4$(for $T_{i,j,k,p}$) $+ m^3$(for $H_{i,j,k}$) $+ m^2$(for $J_{i,j}$) $+ m$(for $C_i$) $= 5^4 + 5^3 + 5^2 + 5 = 780$.

The results given in Figs. 5, 6, and 7 confirm that the existence of dominant modes in the dynamics of a system can be successfully exploited to construct accurate reduced-order models. However, in the case of chaotic dynamics the accuracy of these reduced-order models is maintained only over a finite time interval and around one given trajectory. This is a consequence of the sensitivity to initial conditions, an intrinsic feature of all chaotic systems. Specifically, if at one given time instant the effect of a nondominant mode is neglected, then that leads to a very small error locally in the state-space trajectory. However, this error grows exponentially in the case of chaotic dynamics, as observed in Fig. 7 where a three-mode model is shown to predict the dynamics only over a short time interval. When more modes are included in the reduced-order model, the time
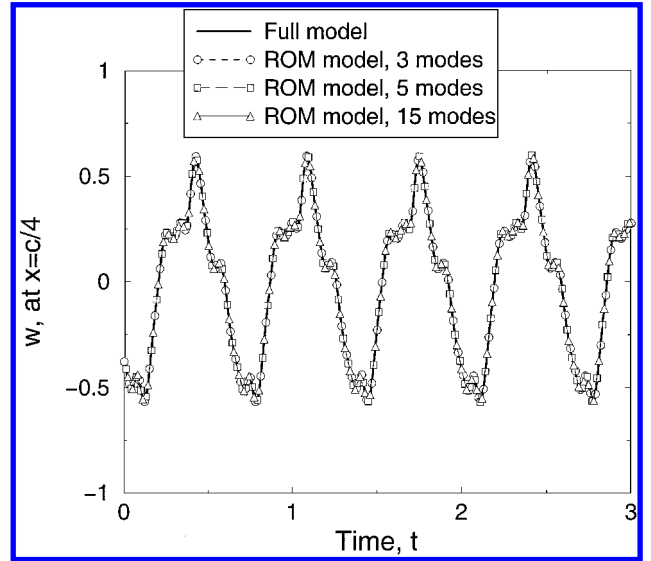


**Fig. 6 Time-marching solution for panel using the full model and three distinct reduced-order models for a case of a panel with limit-cycle oscillations.**
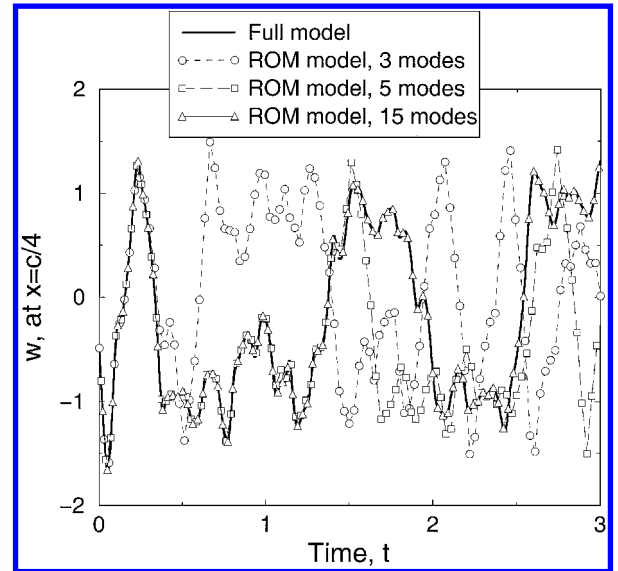


**Fig. 7 Time-marching solution for a panel using the full model and three distinct reduced-order models for a case of a panel with chaotic dynamics.**

interval where model reduction is accurate is increased. In contrast, Fig. 5, shows that reduced-order models are accurate over long time intervals when the dynamics indicates a stable, decaying oscillation. Moreover, reduced-order models are accurate in the case of limit-cycle oscillations, as shown in Fig. 6. In all these calculations the difference between the dynamics predicted by the full model and the reduced-order models is less than 5%.

The presence of sensitivity to initial conditions and chaotic dynamics can limit the applicability of reduced-order models in predicting globally the dynamics of a system. However, reduced-order models can successfully be used in a local fashion. In many applications, such as chaos suppression, targeting, or limit-cycle stabilization, the models used to predict the dynamics of the system do not have to be globally accurate over the entire state space. Typically, these models are required to be accurate only locally, along one trajectory of the system.[26] Thus, reduced-order modeling can be successfully used for local modeling as well as local system identification. The local system identification method[26] is an identification technique designed for determining the dynamical models of systems undergoing limit-cycle oscillations. For example, Fig. 4 shows
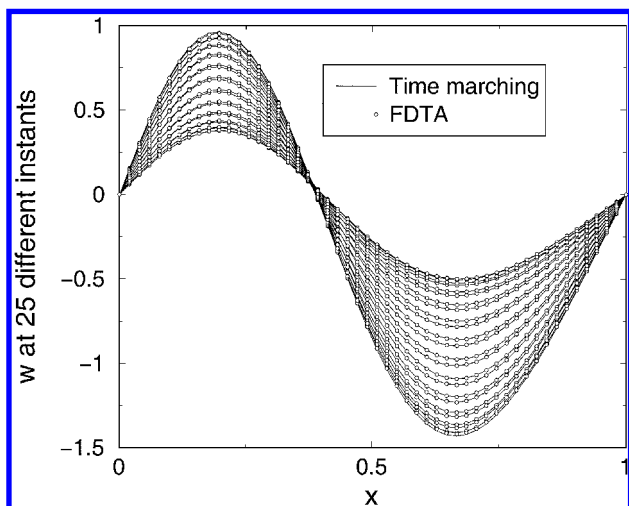
**Fig. 8   Limit-cycle oscillations computed using time marching and the FDTA for a panel forced with unsteady loads with zero structural nonlinearity ($G = 0$).**
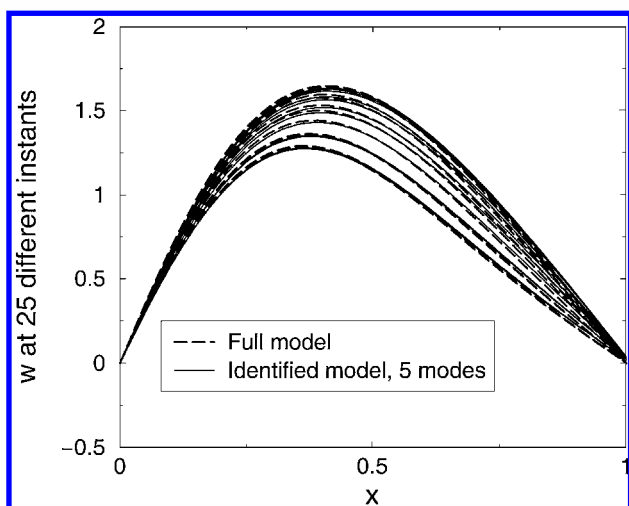


**Fig. 9   Limit-cycle oscillations computed using the FDTA for the full nonlinear model and an identified nonlinear reduced-order model of a panel forced with unsteady aerodynamics.**

that the combined reduced-order modeling and system identification are accurate models in the case of a limit-cycle oscillation. In all of these calculations, an error less than 5% is obtained. In addition, the FDTA presented in the previous section can be used to compute limit-cycle oscillations for both the cases of stable or unstable oscillations as well as limit-cycle oscillations.

Both the full model and the identified POD model are used to apply the FDTA for computing limit-cycle oscillations. The linearized response of the panel (for $G = 0$) forced by the unsteady loading is shown in Fig. 8. The FDTA is applied also to the nonlinear aeroelastic model of the flow and panel, and the results are shown in Fig. 9. For both the linear and nonlinear case the shapes of the panel at 25 successive time instants during one period of the oscillations are presented. The identified reduced-order aeroelastic model is also used in conjunction with the FDTA. Good agreement in predicting the limit-cycle behavior (e.g., amplitude and spatial shape) between the reduced-order and the full models is obtained, as shown in Fig. 9. In all of the results presented in Figs. 8 and 9, the difference between the dynamics predicted by the full model and the computed and identified reduced-order models is less than 5%.

## Features of the Finite Difference in Time Approach

Several advantages of the FDTA as compared to the fast Galerkin and the alternating frequency-time domain techniques were noted. One of the important advantages is that the computation time

required by the FDTA grows linearly with $N$ instead of $N^2 \log N$ or $N^2$ as in other methods. The growth is linear because only systems of linear equations with bidiagonal and tridiagonal matrices have to be solved at each iteration step. Also, the method works for autonomous as well as nonautonomous forced systems and is equally applicable to problems where subharmonics or superharmonics are to be calculated.

The FDTA resembles the alternating time-frequency method,[20,52,53] but it is significantly different, for example, the basis functions used are fundamentally different. The basis functions for the FDTA are interpolation functions, as distinct from sinusoidal functions. Also, the technique for computing time derivatives is different, and the FDTA operates and iterates in the time domain only, rather than alternating between time and frequency domains.

The FDTA can be used to handle complex nonlinearities. However, the complexity of the nonlinearity is transferred to the nonlinear solver to some extent. Thus, the stronger and more complex the nonlinearities are, the less robust the available nonlinear solvers are likely to be. Nevertheless, the current method is not limited to piecewise linear nonlinearities such as the method proposed by Choi and Noah.[51]

The FDTA can use basis functions where the time sampling is not uniform, as distinct from most FFT-based approaches. The nonuniformity of the time samples is a distinct advantage in those applications where the dynamics must be resolved more finely only in certain parts of the limit cycle and not uniformly throughout the entire period of oscillation.

A Newton–Raphson iterative method has been applied to the numerical equations obtained via the FDTA, and a fast and easy to implement algorithm has been presented, providing a useful and general tool for studying complex nonlinear dynamic systems. The novel contribution of the method proposed is not the use of the Newton–Raphson method per se, but rather the idea of using alternative basis functions when approximating the shape of the limit cycle. Also, the derivatives required for the implementation of the FDTA can be precomputed, and a general expression for the residual vector can be obtained without extensive analytical or numerical work. Moreover, the method proposed herein can be used in conjunction with the solution algorithm presented by Leung and Ge[61] because most symmetrical finite difference formulations used in the FDTA lead to a Toeplitz structure of the Jacobian. However, it is not the purpose of the present paper to discuss the applicability or robustness of various nonlinear solvers. To implement the FDTA, any iterative or direct solution algorithm can be used, although the direct solvers typically require a large storage during computations. In the numerical examples presented, we used Newton–Raphson iterations. Methods such as pseudo-time marching, Broyden method, or other iterative methods can be used as well.

## Conclusions

A low-dimensional model of the spatial distribution of a buffeting panel was constructed starting from a high-dimensional model by means of model reduction using POD. The time evolution/dynamics of the panel forced by an aerodynamic load was modeled and identified by means of a system identification. The dynamics of the identified reduced-order models was compared to the dynamics of the full model, and good performance of the models, as well as the identification procedure, was found. Limit-cycle oscillations were computed and modeled using the FDTA and POD.

The local system identification method was shown to provide accurate and useful results when combined with model reduction. The principal factor limiting the highest dimension of the system to be analyzed is the number of parameters of the model to be identified. The critical factor affecting the performance of the identified reduced-order model is the accuracy achieved in the calculation of the dominant coherent structures.

## Acknowledgments

# References

[1] Dowell, E. H., and Hall, K. C., "Modeling of Fluid-Structure Interaction," *Annual Reviews of Fluid Mechanics*, Vol. 33, No. 1, 2001, pp. 445–490.

[2] Epureanu, B. I., and Dowell, E. H., "Reduced Order System Identification of Nonlinear Aeroelastic Systems," *Proceedings of the First M.I.T. Conference on Computational Fluid and Solid Mechanics*, Vol. 1, edited by K. J. Bathe, Elsevier, Cambridge, MA, 2001, pp. 1152–1160.

[3] Borri, M., and Bottasso, C., "Ptrov-Galerkin Finite Elements in Time for Rigid-Body Dynamics," *Journal of Guidance, Control, and Dynamics*, Vol. 17, No. 5, 1994, pp. 1061–1068.

[4] Milgram, J. H., and Chopra, I., "Air Resonance of Hingeless Rotor Helicopters in Trimmed Forward Flight," *Journal of the American Helicopter Society*, Vol. 39, No. 4, 1994, pp. 46–59.

[5] Tamma, K. K., Chen, X., and Sha, D., "Further Developments Towards a New Virtual-Pulse Time Integral Methodology for General Non-Linear Transient Thermal Analysis," *Communications in Numerical Methods in Engineering*, Vol. 10, No. 12, 1994, pp. 961–971.

[6] Tamma, K. K., Zhou, X., and Sha, D., "Towards a Formal Theory of Development/Evolution and Characterization of Time Discretized Operators for Heat Transfer," *International Journal of Numerical Methods for Heat and Fluid Flow*, Vol. 9, No. 3, 1999, pp. 348–380.

[7] Tamma, K. K., Zhou, X., and Sha, D., "A Theory of Development and Design of Generalized Integration Operators for Computational Structural Dynamics," *International Journal for Numerical Methods in Engineering*, Vol. 50, No. 7, 2001, pp. 1619–1668.

[8] Wang, Y., "Stick-Slip Motion of Frictionally Damped Turbine Airfoils: A Finite Element in Time (FET) Approach," *Journal of Vibration and Acoustics*, Vol. 119, No. 4, 1997, pp. 236–242.

[9] Warner, M. S., and Hodges, D. H., "Solving Boundary-Value Problems Using hp-Version Finite Elements in Time," *International Journal for Numerical Methods in Engineering*, Vol. 43, No. 1, 1998, pp. 425–440.

[10] Warner, M. S., and Hodges, D. H., "Solving Optimal Control Problems Using hp-Version Finite Elements in Time," *Journal of Guidance, Control, and Dynamics*, Vol. 23, No. 1, 2000, pp. 86–95.

[11] Noor, A. K., "Recent Advances and Applications of Reduction Methods," *Applied Mechanics Review*, Vol. 47, No. 5, 1994, pp. 125–145.

[12] Stone, E., and Cutler, A., "Introduction to Archetypal Analysis of Spatio-Temporal Dynamics," *Physica D*, Vol. 96, No. 1, 1996, pp. 110–131.

[13] Sirovich, L., "Turbulence and the Dynamics of Coherent Structures, Part I: Coherent Structures," *Quarterly of Applied Mathematics*, Vol. XLV, No. 3, 1987, pp. 561–571.

[14] Sirovich, L., "Turbulence and the Dynamics of Coherent Structures, Part II: Symmetries and Transformations," *Quarterly of Applied Mathematics*, Vol. XLV, No. 3, 1987, pp. 573–582.

[15] Sirovich, L., "Turbulence and the Dynamics of Coherent Structures, Part III: Dynamics and Scaling," *Quarterly of Applied Mathematics*, Vol. XLV, No. 3, 1987, pp. 583–590.

[16] Holmes, P., Lumley, J. L., and Berkooz, G., *Turbulence, Coherent Structures, Dynamical Systems and Symmetry*, 1st ed., Cambridge Univ. Press, Cambridge, England, U.K., 1996, p. 144.

[17] Liu, Z. C., Adrian, R. J., and Hanratty, P., "Reynolds Number Similarity of Orthogonal Decomposition of the Outer Layer of Turbulent Wall Flow," *Physics of Fluids*, Vol. 6, No. 8, 1994, pp. 2815–2819.

[18] Shaw, S. W., and Pierre, C., "Normal Modes of Vibration for Non-Linear Continuous Systems," *Journal of Sound and Vibration*, Vol. 169, No. 3, 1994, pp. 319–347.

[19] Pierre, C., Ferri, A. A., and Dowell, E. H., "Multi-Harmonic Analysis of Dry Friction Damped Systems Using an Incremental Harmonic Balance Method," *Journal of Applied Mechanics*, Vol. 52, No. 2, 1985, pp. 958–964.

[20] Ling, F. H., and Wu, X. X., "Fast Galerkin Method and Its Application to Determine Periodic Solutions of Non-Linear Oscillators," *International Journal for Non-Linear Mechanics*, Vol. 22, No. 2, 1987, pp. 89–98.

[21] Guckenheimer, J., and Holmes, P., *Nonlinear Oscillations, Dynamical Systems, and Bifurcations of Vector Fields*, Springer-Verlag, New York, 1983.

[22] Moon, F. C., *Chaotic and Fractal Dynamics: an Introduction for Applied Scientists and Engineers*, Wiley, New York, 1992, p. 180.

[23] Ott, E., *Chaos in Dynamical Systems*, Cambridge Univ. Press, New York, 1993, p. 25.

[24] Strogatz, S. H., *Nonlinear Dynamics & Chaos*, Addison Wesley Longman, Reading, MA, 1994, p. 196.

[25] Wiggins, S., *Introduction to Applied Nonlinear Dynamical Systems and Chaos*, Springer-Verlag, New York, 1990, p. 289.

[26] Epureanu, B. I., and Dowell, E. H., "System Identification for Ott-Grebogi-Yorke Controller Design," *Physical Review E*, Vol. 56, No. 5, 1997, pp. 5327–5331.

[27] Epureanu, B. I., and Dowell, E. H., "On the Optimality of the OGY Control Scheme," *Physica D*, Vol. 116, No. 1–2, 1998, pp. 1–7.

[28] Epureanu, B. I., Trickey, S. T., and Dowell, E. H., "Stabilization of Unstable Limit Cycles in Systems with Limited Controllability: Expanding the Basin of Convergence of OGY-type Controllers," *Nonlinear Dynamics*, Vol. 15, No. 2, 1998, pp. 191–205.

[29] Gilli, M., and Maggio, M., "Predicting Chaos Through an Harmonic Balance Technique: an Application to the Time-Delayed Chua's Circuit," *IEEE Transactions on Circuits and Systems*, Vol. 43, No. 1, 1996, pp. 872–874.

[30] Basso, M., Genesio, R., and Tesi, A., "A Frequency Method for Predicting Limit Cycle Bifurcations," *Nonlinear Dynamics*, Vol. 13, No. 4, 1997, pp. 339–360.

[31] Cunningham, W. J., *Introduction to Nonlinear Analysis*, McGraw–Hill, New York, 1958, p. 171.

[32] Garcia-Margallo, J., and Bejarano, J. D., "The Limit Cycles of the Generalized Rayleigh-Lienard Oscillator," *Journal of Sound and Vibration*, Vol. 156, No. 2, 1992, pp. 283–301.

[33] Piccardi, C., "Bifurcations of Limit Cycles in Periodically Forced Nonlinear Systems: the Harmonic Balance Approach," *IEEE Transactions on Circuits and Systems*, Vol. 41, No. 1, 1994, pp. 315–320.

[34] Piccardi, C., "Harmonic Balance Analysis of Codimension-Two Bifurcations in Periodic Systems," *IEEE Transactions on Circuits and Systems*, Vol. 43, No. 1, 1996, pp. 1015–1018.

[35] Hahn, E. J., and Chen, P. Y. P., "Harmonic Balance Analysis of General Squeeze Film Damped Multi Degree-of-Freedom Rotor Bearing Systems," *Journal of Tribology*, Vol. 116, No. 1, 1994, pp. 499–507.

[36] Higuchi, K., and Dowell, E. H., "Effect of Constant Transverse Force on Chaotic Oscillations of Sinusoidally Excited Buckled Beam," *International Journal of Non-Linear Mechanics*, Vol. 26, No. 3–4, 1991, pp. 419–426.

[37] Lee, M. R., Padmanabhan, C., and Singh, R., "Dynamic Analysis of a Brushless d.c. Motor Using a Modified Harmonic Balance Method," *Journal of Dynamic Systems, Measurement and Control*, Vol. 117, No. 1, 1995, pp. 283–291.

[38] Matsuzaki, Y., "Reexamination of Stability of a Two-Dimensional Finite Panel Exposed to an Incompressible Flow," *Journal of Applied Mechanics*, Vol. 48, No. 3, 1981, pp. 472–478.

[39] Yuen, S. W., and Lau, S. L., "Effects of In-Plane Load on Nonlinear Panel Flutter by Incremental Harmonic Balance Method," *AIAA Journal*, Vol. 29, No. 9, 1991, pp. 1472–1479.

[40] Hall, K. C., Thomas, J. P., and Clark, W. S., "Computation of Unsteady Nonlinear Flows in Cascades Using a Harmonic Balance Technique," *AIAA Journal*, Vol. 40, No. 5, 2002, pp. 879–886.

[41] Ferri, A. A., "On the Equivalence of the Incremental Harmonic Balance Method and the Harmonic Balance-Newton Raphson Method," *Journal of Applied Mechanics*, Vol. 53, No. 1, 1986, pp. 455–457.

[42] Lau, S. L., and Zhang, W. S., "Nonlinear Vibrations of Piecewise-Linear Systems by Incremental Harmonic Balance Method," *Journal of Applied Mechanics*, Vol. 59, No. 1, 1992, pp. 153–160.

[43] Pierre, C., and Dowell, E. H., "A Study of Dynamic Instability of Plates by an Extended Incremental Harmonic Balance Method," *Journal of Applied Mechanics*, Vol. 52, No. 5, 1985, pp. 693–697.

[44] Chaisomphob, T., Kanok-Nukulchai, W., and Nishino, F., "An Automatic Arc Length Control Algorithm for Tracing Equilibrium Paths of Nonlinear Structures," *Proceedings of JSCE, Journal of Earthquake Engineering*, Vol. 5, No. 1, 1988, pp. 227–230.

[45] Holodniok, M., and Kubicek, M., "DERPER—An Algorithm for the Continuation of Periodic Solutions in Ordinary Differential Equations," *Journal of Computational Physics*, Vol. 55, No. 1, 1984, pp. 254–267.

[46] Lau, S. L., Cheung, Y. K., and Wu, S. Y., "Incremental Harmonic Balance Method with Multiple Time Scales for Aperiodic Vibration of Nonlinear Systems," *Journal of Applied Mechanics*, Vol. 50, No. 4, 1983, pp. 871–876.

[47] Moiola, J., and Chen, G., "Computation of Limit Cycles via Higher Order Harmonic Balance Approximation," *IEEE Transactions on Automatic Control*, Vol. 38, No. 1, 1993, pp. 782–790.

[48] Jones, J. C. P., Zhuang, M., and Cankaya, I., "Symbolic Computation of Harmonic Balance Equations," *International Journal of Control*, Vol. 68, No. 3, 1997, pp. 449–460.

[49] Donescu, P., and Virgin, L. N., "Efficient Determination of Higher-Order Periodic Solutions Using n-Mode Harmonic Balance," *Journal of Applied Mathematics*, Vol. 56, No. 1, 1996, pp. 21–32.

[50] Donescu, P., Virgin, L. N., and Wu, J. J., "Periodic Solutions of an Unsymmetric Oscillator Including a Comprehensive Study of Their Stability Characteristics," *Journal of Sound and Vibration*, Vol. 192, No. 5, 1996, pp. 959–976.

[51] Choi, Y. S., and Noah, S. T., "Forced Periodic Vibration of Unsymmetric Piecewise-Linear Systems," *Journal of Sound and Vibration*, Vol. 121, No. 1, 1988, pp. 117–126.

[52] Cameron, T. M., and Griffin, J. H., "An Alternating Frequency/Time Domain Method for Calculating the Steady-State Response of Nonlinear Dynamic Systems," *Journal of Applied Mechanics*, Vol. 56, No. 3, 1989, pp. 149–154.

[53] Aprile, A., Benedetti, A., and Trombetti, T., "On Non-Linear Dynamic Analysis in the Frequency Domain: Algorithms and Applications," *Earthquake Engineering and Structural Dynamics*, Vol. 23, No. 1, 1994, pp. 363–388.

[54] Epureanu, B. I., Hall, K. C., and Dowell, E. H., "Reduced Order Models of Unsteady Transonic Viscous Flows in Turbomachinery," *Journal Fluids and Structures*, Vol. 18, No. 8, 2000, pp. 1215–1235.

[55] Epureanu, B. I., Hall, K. C., and Dowell, E. H., "Reduced Order Models of Unsteady Viscous Flows in Turbomachinery Using Viscous-Inviscid Coupling," *Journal Fluids and Structures*, Vol. 15, No. 2, 2001, pp. 255–276.

[56] Nataraj, C., and Nelson, H. D., "Periodic Solutions in Rotor Dynamic Systems with Nonlinear Supports: A General Approach," *Journal of Sound and Vibration*, Vol. 111, No. 4, 1989, pp. 187–193.

[57] Ren, Y., and Beards, C. F., "A New Receptance-Based Perturbative Multi-Harmonic Balance Method for the Calculation of the Steady State Response of Non-Linear Systems," *Journal of Sound and Vibration*, Vol. 172, No. 5, 1994, pp. 593–604.

[58] Datta, B. N., *Numerical Linear Algebra and Applications*, Brooks/Cole, Pacific Grove, CA, 1995, p. 187.

[59] Hodges, D. H., and Bless, R. R., "Weak Hamiltonian Finite Element Method for Optimal Control Problems," *Journal of Guidance, Control, and Dynamics*, Vol. 14, No. 1, 1991, pp. 148–156.

[60] Dowell, E. H., and Ilgamov, M., *Studies in Nonlinear Aeroelasticity*, 1st ed., Springer-Verlag, New York, 1988, p. 163.

[61] Leung, A. Y. T., and Ge, T., "Toeplitz Jacobian Matrix for Nonlinear Periodic Vibration," *Journal of Applied Mechanics*, New York, Vol. 62, No. 1, 1995, pp. 709–717.

**This article has been cited by:**

1. Andrea Mannarino, Paolo Mantegazza. 2014. Nonlinear aeroelastic reduced order modeling by recurrent neural networks. *Journal of Fluids and Structures* **48**, 103-121. [CrossRef]

2. James M. Gariffo, Oddvar O. BendiksenEfficient Prediction of Transonic Flutter Boundaries with Linearized Aeroservoelastic Reduced-Order Models . [Citation] [PDF] [PDF Plus]

3. Jeffrey Thomas, Earl Dowell, Kenneth HallUsing Automatic Differentiation to Create a Nonlinear Reduced Order Model of a Computational Fluid Dynamic Solver . [Citation] [PDF] [PDF Plus]

4. Oleg V. Shiryayev, Joseph C. Slater. 2006. Aeroelastic System Identification Using the Minimum Model Error Method. *Journal of Guidance, Control, and Dynamics* **29**:4, 936-943. [Citation] [PDF] [PDF Plus]

5. Oleg Shiryayev, Joseph SlaterEffects of Proper Orthogonal Decomposition on Identification Using the Minimum Model Error Algorithm . [Citation] [PDF] [PDF Plus]

6. Oleg V. Shiryayev, Joseph C. Slater. 2006. Panel Flutter Model Identification Using the Minimum Model Error Method on the Forced Response Measurements. *Journal of Vibration and Acoustics* **128**, 635. [CrossRef]

7. P.J. Attar, E.H. Dowell. 2005. A reduced order system ID approach to the modelling of nonlinear structural behavior in aeroelasticity. *Journal of Fluids and Structures* **21**, 531-542. [CrossRef]